npj | biological timing and sleep

Article

https://doi.org/10.1038/s44323-026-00089-x

The importance of meal timing for maintenance of daily rhythms in the gut transcriptome and microbiota

Felicity K. Hunter[1,2,3], Polly Downton[1,3], Andrea Luengas-Martinez[1,3], Suzanna H. Dickson[1,3], Jafar Cain[1,3], Kathryn J. Else[1,2], Matthew R. Hepworth[1,2] & Julie E. Gibbs[1,2,3] ✉

Gut function exhibits 24 h (circadian) rhythmicity, in part driven by intrinsic clocks within intestinal epithelial cells (IECs). The gut microbiome also demonstrates circadian rhythms in composition and function, important for maintenance of metabolic, immune and gut health. Here, we determined the influence of feeding behaviour on the 24 h colonic landscape using an interval feeding paradigm, whereby food intake was partitioned equally across the 24 h day. RNAseq analysis revealed that the IEC intrinsic clock persists in the absence of diurnal feeding rhythms; however, a subset of key transcripts loses rhythmicity, demonstrating that cell extrinsic temporal cues contribute significantly to the maintenance of the rhythmic gut transcriptome. Furthermore, interval-fed mice demonstrated a striking loss of rhythms in secretory IgA, a critical regulator of the temporal landscape of the gut microbiome. In keeping, rhythmicity within the microbiota and microbial-derived short chain fatty acids was significantly diminished. This work highlights the importance of daily rhythms in feeding behaviour for the maintenance of rhythmic processes within the gut, with implications for metabolic and immune health.

The circadian clock is an intrinsic timer that regulates biological processes to align with the 24 hour (24 h) day. In mammals, light information is conveyed to the central clock within the hypothalamus via the retino-hypothalamic tract, thereby tuning it to daily light–dark cycles[1]. In turn, the central clock coordinates peripheral clocks, found in most cells and tissues around the body, via non-photic *zeitgebers* (meaning time givers), including neuronal signals, hormones, temperature and food intake[2]. At the molecular level, a handful of core clock genes/proteins (*Bmal1*, *Period1/2*, *Clock*, *Cryptochrome 1/2*, *Nr1d1/2* and *Ror*) form transcriptional translational feedback loops which drive 24 h rhythms in clock-controlled genes to facilitate tissue-specific circadian programmes of rhythmic biology[3,4]. In addition, peripheral cues, including those from the diet, also act to entrain rhythmic biology.

Gastrointestinal (GI) functions, including colonic motility, permeability, localised hormone secretion and immune function, exhibit 24 h rhythmicity[5–7]. Our earlier work[8], and that of others[6,9–12], demonstrates that over 50% of the colonic transcriptome is rhythmic in ad libitum fed mice. At a cellular level, multiple cells within the mucosal compartment and muscularis externa house a robust intrinsic clock[13]. The intestinal epithelial cells (IECs) within the mucosal compartment play a key role in maintaining rhythmicity within the colon. Cell-specific ablation of the IEC clock (via targeted deletion of the core clock gene *Bmal1*) causes widespread loss of 24 h rhythmicity within the colonic transcriptome, although a significant proportion of rhythmic transcripts remain unchanged[14]. This likely reflects the presence of additional timing cells within the colon, but also implicates a role for extrinsic rhythmic signals for driving tissue rhythms independent of the IEC molecular clock. IECs form a single lining layer along the gut and play an important role in maintaining gut homoeostasis[15]. Critically, IECs, along with underlying immune responses (including secretory Immunoglobulin A (IgA)), segregate the gut microbiota from the host and facilitate crosstalk between the microbiome and gut resident immune cells. The gut microbiota exhibits 24 h oscillations in composition, biophysical localisation within the intestine and metabolic outputs[9,16–20]. This daily rhythmicity in the microbiome is important for maintenance of metabolic and immune health[21–23].

Feeding behaviour is highly influential over peripheral clocks[24]. Bouts of feeding usually occur during the active phase of the 24 h cycle, daytime for humans and nighttime for nocturnal rodents. Studies in rodents demonstrate that under reverse feeding cycles, where food availability is restricted to the daytime (and thus misaligned to the active phase), highly metabolic

[1]Centre for Biological Timing, University of Manchester, Manchester, UK. [2]Lydia Becker Institute of Immunology and Inflammation, University of Manchester, Manchester, UK. [3]Division of Integrative Physiology, School of Medical Sciences, Faculty of Biology, Medicine and Health, University of Manchester, Manchester, UK. ✉e-mail: julie.gibbs@manchester.ac.uk

organs such as the liver exhibit altered diurnal rhythms in expression of core clock genes[25,26] and other hepatic transcripts[27], which realign with food availability. Molecular mechanisms by which food intake synchronises clockwork machinery are not fully understood, but feeding-derived signals originating from the host[28,29] and the gut microbiota[30] can reset the clock.

Here, we sought to address the influence of feeding behaviour on the 24 h landscape of the colon using an interval feeding paradigm whereby food intake was partitioned equally across the 24 h day. We focused on the IEC, a key timer cell within the colon and at the interface between the host and gut microbiota. In the absence of diurnal rhythms in feeding behaviour, the core clock mechanism persisted within IECs. However, there was significant reorganisation of transcriptional rhythmicity within the gut, and loss of rhythmicity in secretory IgA, beneficial commensals and short-chain fatty acids. Together these data highlight the importance of feeding behaviour for synchronising the gut clock and sustaining rhythmicity, demonstrating that meal timing is a critical factor for maintenance of gut homoeostasis.

Results

Interval feeding uncouples rhythms of food intake from rhythmic behaviours and outputs

To determine the influence of diurnal feeding behaviour on the IEC clock and the 24 h IEC transcriptome, we established an interval feeding regimen. Mice were provided with eight small meals a day at 3 hourly intervals for 16 days (Fig. 1A). This resulted in an equal spread of food consumption across each mealtime (Fig. 1B). In contrast, ad libitum fed mice consumed the majority of their food at night, with ~21% of their food eaten during the light period, as expected (Fig. 1B). During the early acclimatisation period (days 1 and 2), daily food intake was reduced under interval feeding (Supplementary Fig. 1A). However, mice quickly adapted to the regimen, consuming similar amounts of food each day, and consistently consuming 12–13% of total daily intake at each meal. Whilst ad libitum fed mice gained weight (~8%) over the experimental period, interval fed mice maintained their starting weight (Supplementary Fig. 1B, C). Daily activity and metabolic parameters were analysed using the PhenoMaster system. Activity transiently spiked at mealtimes both in interval fed and ad libitum fed mice (co-housed within the same light-tight cabinet) (Fig. 1C). Nevertheless, under both feeding regimens, mice were predominantly active during the night, demonstrating maintenance of nocturnal behaviour. Similarly, drinking activity was greater in the night versus day (Fig. 1D). Oxygen consumption (VO_2), carbon dioxide production (VCO_2) and heat production transiently spiked during mealtimes in interval fed mice, but in keeping with ad libitum fed controls, increased at the onset of the dark phase (Supplementary Fig. 1D–F). The respiratory exchange ratio (RER) dipped during the onset of night in interval fed mice, indicating a shift in fuel source from carbohydrates towards fatty acids, but increased transiently when meals were consumed (reflective of maintained nocturnal activity, but reduced food intake during the dark period) (Fig. 1E). Finally, circulating levels of the circadian hormone corticosterone remained rhythmic with a peak at the onset of the dark phase under both feeding regimens (Fig. 1F). To summarise, mice maintained 24 h rhythms in behavioural activity and corticosterone levels under interval feeding, further supporting the effectiveness of an interval feeding protocol to uncouple rhythms of food intake from other rhythmic behaviours and outputs[31–36]. These data shed new light on the influence of interval feeding on metabolic parameters, revealing that overall metabolic rate was not perturbed.

Interval feeding drives temporal reorganisation of the IEC transcriptome, despite persistence of the cellular molecular clock

We utilised the interval feeding paradigm to reveal how the IEC 24 h transcriptome responds to loss of diurnal feeding behaviour. IECs (~80% purity, Supplementary Fig. 2A) were harvested across the 24 h day from interval fed mice and ad libitum controls for RNAseq analysis. Interval feeding drove substantial reorganisation of 24 h rhythms in gene expression (Fig. 2A, Supplementary Data 1). Whilst 3662 transcripts were similarly rhythmic under both regimens (same, Supplementary Fig. 2A), a proportion (217 transcripts) demonstrated a change in rhythmicity (altered amplitude and/or phase, Fig. 2B), whilst others gained (418 transcripts) or lost (1237 transcripts) rhythmicity. Of note, ~25% of the IEC transcriptome lost rhythmicity under interval feeding. Loss and gain of rhythmicity were not owing to changes in overall expression levels (Supplementary Fig. 2C), indicating that transcript oscillation is regulated independently of the magnitude of expression. Furthermore, analysis of the two feeding regimens (independent of sample collection time) revealed no differentially expressed genes (DESeq2 analysis, padj < 0.1, data not shown). This indicates that the temporal dynamics of transcription, but not the transcriptional programmes themselves, are altered by interval feeding.

Examination of the changed transcript subset revealed that in ad libitum fed mice, expression peaked predominantly at the transition from light to dark (prior to the onset of activity and increased food intake). Under interval feeding, this phasing was re-distributed across the 24 h day (Fig. 2C). Further analysis mapped these changed transcripts onto pathways including "Circadian rhythms", "Steroid biosynthesis" (including *Fdft1*, *Sqle* and *Cyp51*), "Bile secretion" (including *Ldlr* and *Hmgcr*) and "Mineral absorption" (including *Mt1/2* and *Atp1a1*) (Fig. 2D and E, Supplementary Figs. 2D and 3). Importantly, the majority of core clock genes fell into the change group with *Per1/2/3*, *Cry1/2*, *Arntl (Bmal1)*, *Dbp* and *Rorc* exhibiting robust 24 h rhythms under interval feeding. However, these rhythms were phase advanced by 2–4 h (with the exception of *Clock*), and thus misaligned with observed activity and hormonal rhythms (Fig. 2F and G and Supplementary Fig. 2E). Similar shifts in clock gene phase were observed in the liver (Supplementary Fig. 4), comparable to findings by others employing similar feeding regimens[31]. Thus, the IEC clock persists in the absence of diurnal rhythms in feeding behaviour, but rhythmic feeding provides temporal cues that synchronise this timer to the light–dark cycle.

Diurnal feeding behaviour delivers rhythmic cues important for maintenance of 24 h oscillations in the IEC transcriptome

The observed loss and gain of rhythmicity in subsets of transcripts under interval feeding, despite the intact clockwork machinery, demonstrates dependence on rhythmic cues delivered by diurnal feeding behaviour. This observation provides new insight into the relative importance of extrinsic temporal cues and intrinsic clocks in the maintenance of a rhythmic gut transcriptome. Transcripts that gained rhythmicity under interval feeding tended to peak during the middle of the day (ZT6-8) (Fig. 3A and B) and could be mapped to a small number of pathways, including "Glycerophospholipid metabolism" (including *Pla2g12a* and *Lpin2*) and "Ether lipid metabolism" (including *Plpp3* and *Pld2*) (Fig. 3C and D).

Transcripts that lost rhythmicity tended to peak under ad libitum conditions at either the end of the night (ZT20-22) or the end of the day (ZT8-10) (Fig. 3E and F). Enrichment analysis did not yield any significant common biological pathways (using adj.$P < 0.05$), less stringent analysis (using $P < 0.05$, Supplementary Fig. 5A) did identify pathways including "Citrate cycle" and "Lysine degradation". Analysis of upstream regulators (IPA analysis, Fig. 3G) identified a number of endogenous chemicals, including the fatty acids palmitic acid and palmitoleic acid, and cholesterol and cholesterol metabolites. This raises the possibility that organic compounds could act as *zeitgebers*, important for maintaining daily rhythms within the gut transcriptome. Additionally, sterol regulatory element binding transcription factor (SREBF) 1 and 2 were identified as transcriptional regulators of genes that lost rhythmicity (Fig. 3G). SREBF1/2 are noted for their circadian rhythmicity in expression levels and activity, driven in part by feeding-fasting cycles[37–39]. Expression of *Srebf1* exhibited 24 h rhythmicity in IECs under ad libitum feeding (peaking during the active phase), which was lost under interval feeding (Supplementary Fig. 5B).

Diurnal feeding behaviour is required for rhythmic IgA secretion

IgA plays a major role in host regulation of the microbiota, and its production by intestinal plasma cells is supported by IECs. Furthermore, we

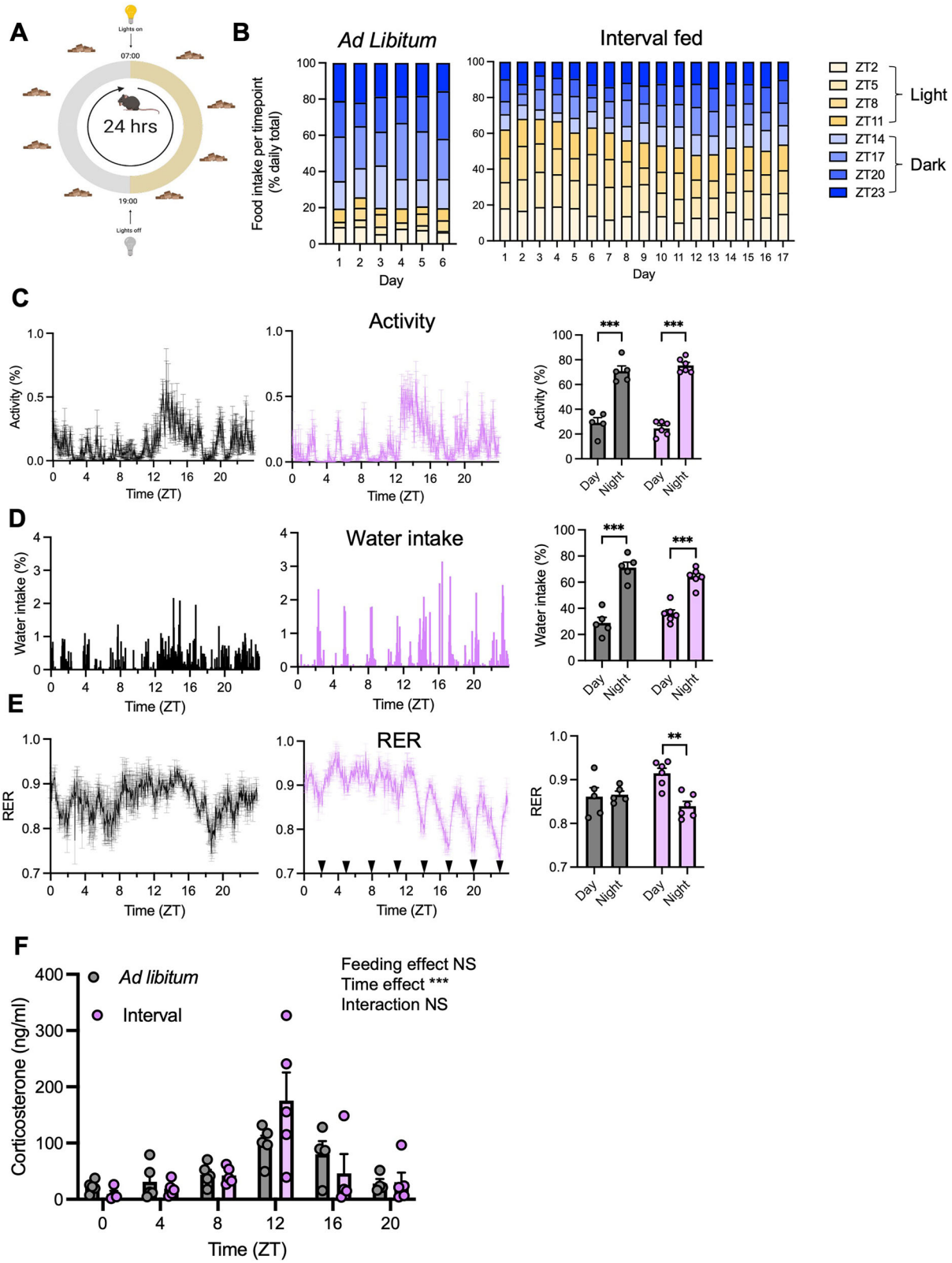

Fig. 1 | Effects of interval feeding on food intake and rhythmic physiology. **A** Schematic illustrating the interval feeding schedule. Mice were maintained under a 12:12 light–dark cycle and provided access to food for a short window of time every 3 h. **B** Quantification of food intake at every mealtime. Food intake per cage (5 animals per cage, averaged over 3 cages (ad libitum fed) or 6 cages (interval fed)), expressed as a percentage of the day's total intake. Phenomaster cages were utilised to measure (in singly housed mice): **C** activity; **D** water intake and **E** respiratory exchange rate (RER) under ad libitum feeding (black) and interval feeding (purple). Line plots show group average ($n = 6$ interval fed, $n = 5$ ad libitum fed), meal times denoted by triangles. Bar charts quantify partitioning into day (12 h lights on) and night (12 h lights off), two-way ANOVA and post-hoc Tukey's multiple comparisons test. **F** Circulating corticosterone levels in ad libitum fed mice ($n = 4$–5/time point) and interval fed mice ($n = 4$–5/time point), two-way ANOVA. See also Supplementary Fig. 1.

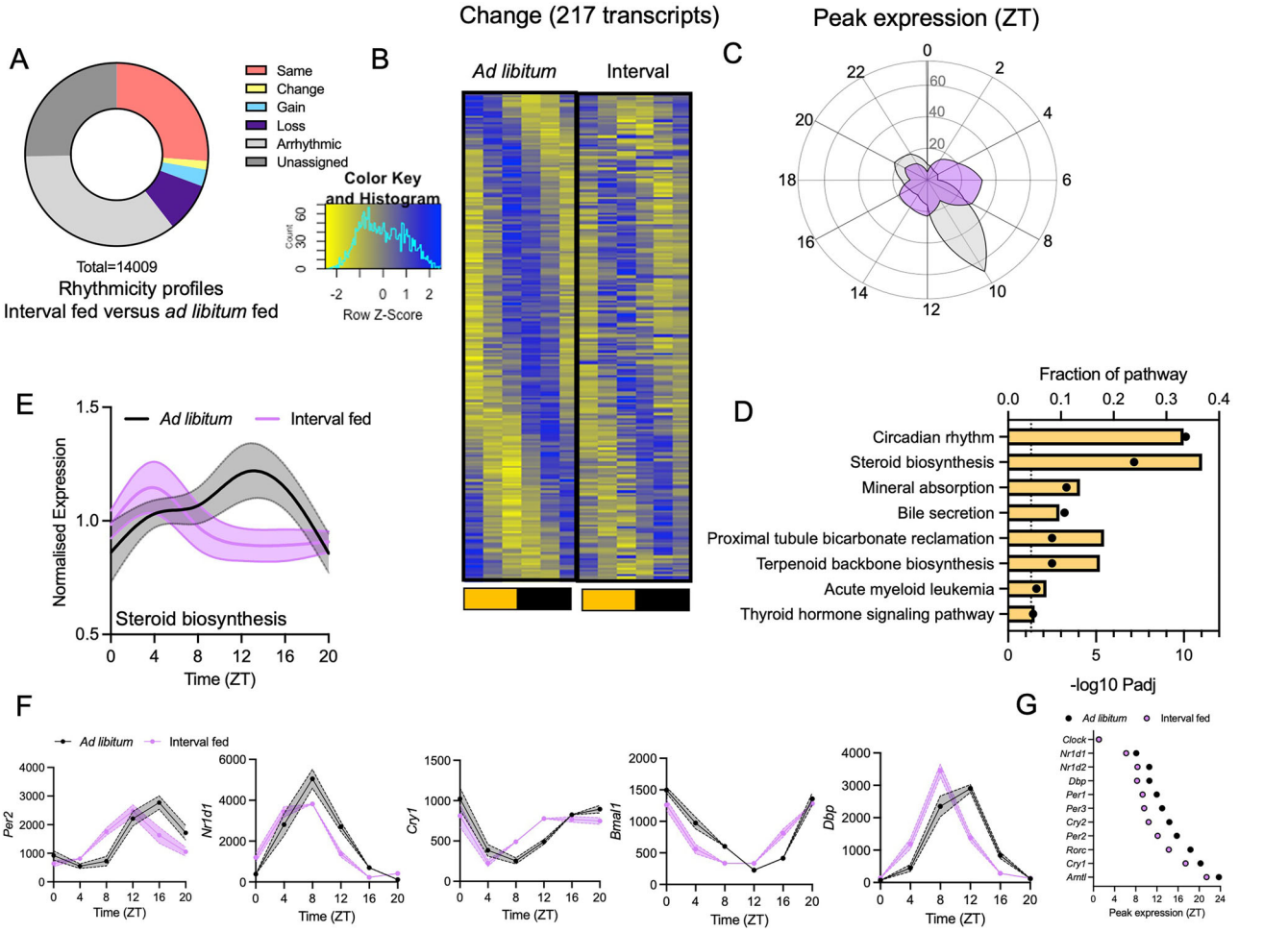

Fig. 2 | The IEC clock persists under interval feeding. **A** Proportion of the IEC transcriptome showing 24 h rhythms under both ad libitum and interval feeding ("same" or "change"); under ad libitum feeding only ("loss"); or under interval feeding only ("gain"). 24 h rhythmicity assessed using CompareRhythms. **B** Transcripts demonstrating changed rhythmicity under interval feeding, $n = 4–5$/time point, 6 time points per condition. **C** Temporal distribution of the peak expression of transcripts demonstrating changed rhythmicity, grey = ad libitum and purple = interval fed. **D** Pathway analysis (mouse KEGG 2019) of transcripts assigned a change in rhythmicity. Bars quantify the fraction of the pathway represented, and dots represent statistical significance (dotted line marks Padj = 0.05). **E** Spline plot of normalised expression of all genes in the "Steroid biosynthesis" pathway, which appeared in our data (Mmu 00100; 17 genes), error bars represent 95% CIs around the mean. **F** Expression of clock genes (normalised expression) over time, which were assigned changed rhythmicity, $n = 4–5$/time point. **G** Phasing of clock gene expression within the IECs (as determined by CompareRhythms) under ad libitum or interval feeding. See also Supplementary Figs. 2 and 3.

previously demonstrated that rhythms in IgA (generated in response to feeding) impact the gut microbiota. Whilst some components of this pathway maintained 24 h rhythms in IECs (*Itga4*, *Tnfsf13* and *Itgb7*), others lost (*Tgfb1*, *Ltbr*) or gained (*Il15ra*) rhythmicity (Fig. 3H). Interestingly, *Pigr* (encoding PIgR protein, which facilitates IgA transport across epithelial cells) was highly expressed in IECs, but did not exhibit 24 h rhythmicity under either feeding regimen. Altogether, these findings suggest that IECs may play further roles in facilitating the IgA response in a rhythmic manner. This prompted exploration of the impact of interval feeding on faecal IgA, which revealed a striking loss of 24 h rhythms in IgA secretion (Fig. 3I).

Diurnal feeding is important for maintenance of rhythms in the microbiome

Given the importance of 24 h rhythmicity in both IECs and IgA production for maintenance of the rhythmic microbiota[9,22,40], we examined the response of the gut microbiota to interval feeding. 16s rRNAseq analysis was performed on faecal samples collected around the clock in ad libitum and interval fed mice. Analysis of alpha diversity (Shannon index, a measure of species richness and evenness) revealed no difference between feeding regimen when all samples were pooled irrespective of collection time (Supplementary Fig. 6A). However, as expected[40] in ad libitum fed mice, alpha diversity exhibited variation over the 24 h day, with a nadir during the rest phase. This persisted under interval feeding (Fig. 4A). Analysis of 24 h rhythmicity in bacterial abundance in ad libitum fed mice revealed 231/477 oscillatory OTUs (relative abundance, JTK_cycle analysis, adj. $P < 0.05$), which was reduced to 98/477 under interval feeding (with an overlap of 48 OTUs) (Fig. 4B–D, Supplementary Data 3). When OTUs were mapped onto phyla, Bacteroidetes and Firmicutes showed the expected anti-phasic relationship under both feeding conditions, with interval feeding inducing a phase advance (Fig. 4E and Supplementary Fig. 6B). OTUs that lost rhythmicity included those assigned to *Lactobacillus gasseri* and *Oscillobacter* (Fig. 4F). Those that gained rhythmicity included *Clostridiales vadin BB60* group (Fig. 4G) and those that remained the same included *Lachnospiraceae* and *Parabacteroides goldsteinii* (Fig. 4H). Thus, these data highlight the importance of diurnal feeding behaviour on the maintenance of a rhythmic microbiota. The microbiota plays a critical role in host metabolism, generating metabolic products from the breakdown of dietary components, with potent effects on the host. As an assessment of microbial outputs, short chain fatty acid (SCFA) levels were quantified across time from the caecum (Fig. 4I and

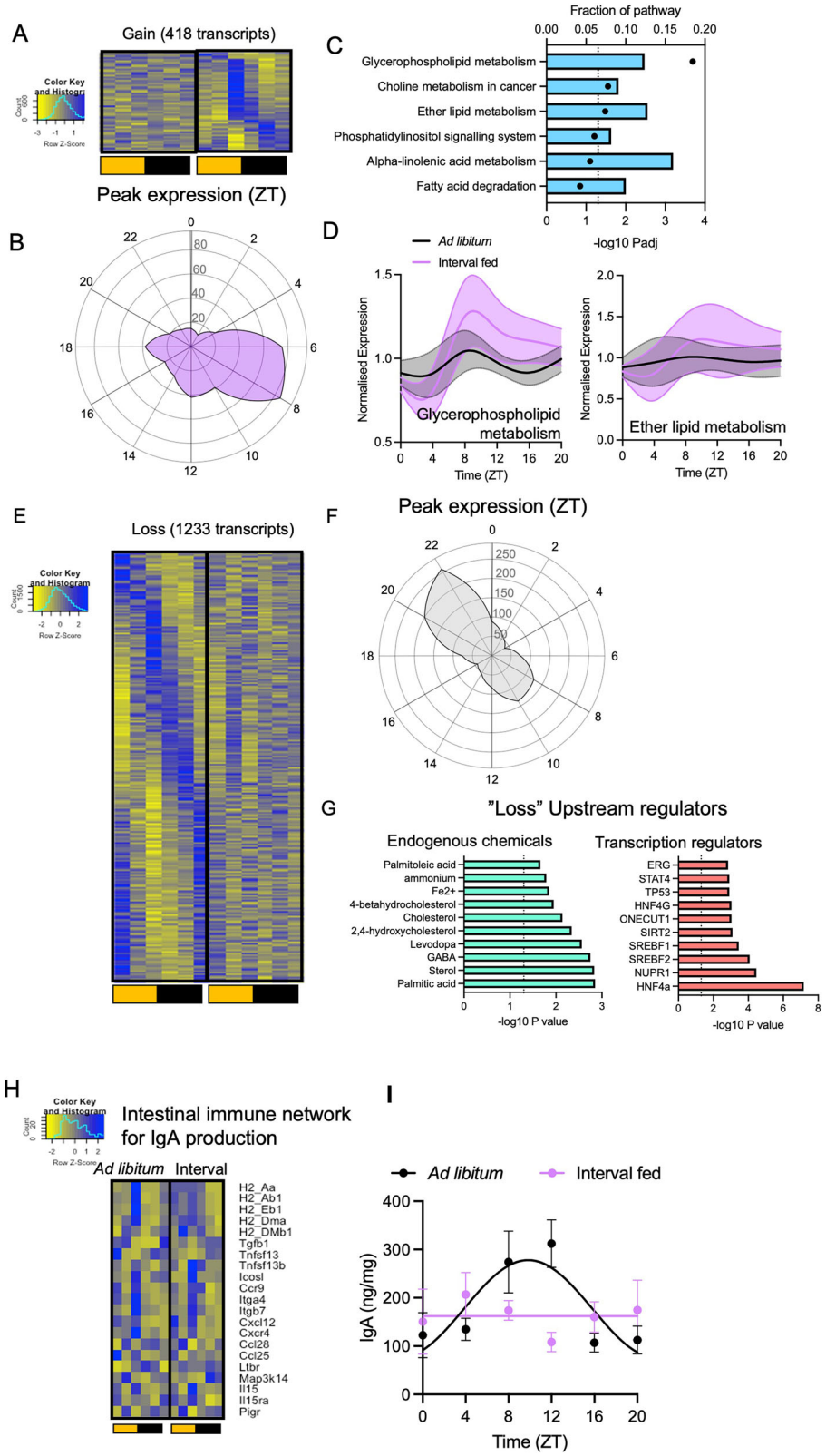

Fig. 3 | Interval feeding drives significant temporal reorganisation of the IEC transcriptome. A 418 transcripts showed a gain of 24 h rhythmicity under interval feeding. **B** Temporal distribution of the peak expression of transcripts that were arrhythmic in ad libitum fed mice but gained 24 h rhythmicity under interval feeding. **C** Pathway analysis (mouse KEGG 2019) of transcripts assigned a gain in rhythmicity. Bars quantify the fraction of the pathway represented, and dots represent statistical significance (dotted line marks Padj = 0.05). **D** Spline plots of mean normalised expression of all genes in the denoted pathways, which appeared in the data and were in the gain category, error bars represent 95% CIs around the mean. Glycerophospholipid metabolism (Mmu_00564, 12 genes) and Ether lipid metabolism (Mmu_00565, 6 genes). **E** 1233 transcripts showed loss of 24 h rhythmicity under interval feeding. **F** Temporal distribution of the peak expression of transcripts that were rhythmic in ad libitum fed mice but arrhythmic under interval feeding. **G** Upstream regulator analysis of IEC transcripts, which lost rhythmicity under interval feeding. The top 10 regulators in the categories "endogenous chemicals" and "transcription regulators" and their significance are shown. **H** Normalised expression across time of genes within the IEC RNAseq data, which were in the KEGG mouse 2019 pathway "Intestinal immune network for IgA production" (mmu_04672; 21 genes), $n = 4–5$/time point. **I** Faecal IgA across time in ad libitum and interval fed animals, $n = 3–5$/time point. Data was tested for fitting to a sine wave with a nonzero baseline and wavelength of 24, and as appropriate, a sine wave or horizontal line was plotted (ad libitum: $P = 0.0017$; interval fed: $P = 0.554$). See also Supplementary Fig. 4.

Supplementary Table 1). Of the five metabolites screened, caproic acid and valeric acid showed 24 h rhythmicity (JTK_cycle, BH.Q < 0.05) in ad libitum fed mice. However, these SCFAs lost rhythmicity in interval fed mice. Together, these data demonstrate significant temporal reorganisation of the bacterial composition of the gut microbiota and its metabolic activity in the absence of diurnal feeding cues.

Discussion

This study demonstrates the importance of diurnal feeding behaviour on maintenance of 24 h rhythmicity and host–microbiota interactions within the GI tract. The IECs house a robust molecular clock, which persists in the absence of diurnal feeding rhythms. Despite minimal disruption to the rhythmic nature of core clock genes, a significant proportion (~25%) of the

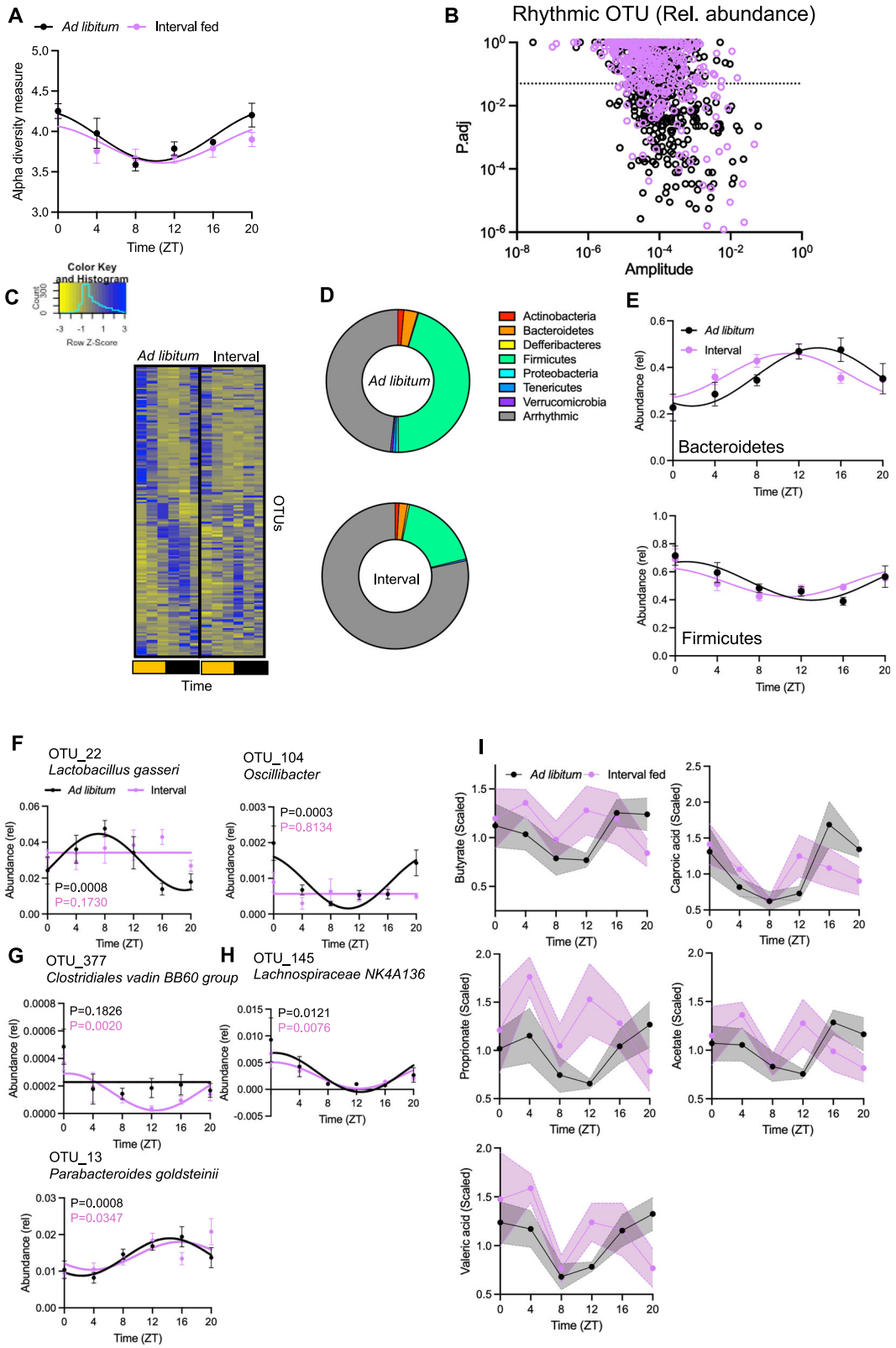

IEC transcriptome lost rhythmicity under interval feeding, implicating reliance on feeding-derived rhythmic *zeitgebers*, which may include fatty acids and sterols. 16s rRNA sequencing, IgA profiling and metabolomic analyses reinforce the notion that feeding behaviour regulates daily rhythms in secretory IgA and within the gut microbiota and its metabolic outputs. Together, this work reveals that meal timing is a critical determinant of microbial rhythmicity and implicates the importance of feeding behaviour in the maintenance of metabolic and immunological processes reliant on a rhythmic microbiota.

Mice with ad libitum access to food do not undergo significant periods of fasting per se; their feeding behaviour is partitioned so that the majority (~75%) of their daily food is consumed during the night. Interval feeding

Fig. 4 | Interval feeding drives loss of rhythmicity in the microbiome. 16s rRNAseq analysis of faecal samples collected across the 24 h day in ad libitum and interval fed mice. **A** Alpha diversity (Shannon Index) plotted across time in ad libitum and interval fed animals, $n = 5$/time point. Data was tested for fitting to a sine wave with a nonzero baseline and wavelength of 24 (ad libitum: $P < 0.0001$; interval fed: $P = 0.0049$). **B** Analysis of 24 h rhythmicity (JTK_Cycle) of all OTUs (total abundance, 477 OTUs) from ad libitum (black) and interval (purple) fed mice. Points falling below the dotted line (P.adj < 0.05) were assigned as rhythmic. **C** Relative abundance of OTUs (ordered by peak phase in ad libitum fed mice) where the mean relative abundance is >0.05%. **D** Taxonomic assignment by Phyla of rhythmic OTUs under the two feeding regimens. **E** Temporal distribution of OTUs (relative abundance) assigned to the two major phyla—Bacteroidetes and Firmicutes. Data was tested for fitting to a sine wave with a nonzero baseline and wavelength of 24 (Bacteroidetes: ad libitum, $P = 0.0004$; interval fed, $P = 0.0002$ and Firmicutes: ad libitum, $P = 0.0010$ and interval fed, $P = 0.0015$). Example OTUs that **F** lost or **G** gained rhythmicity under interval feeding or were **H** unchanged. Data was tested for fitting to a sine wave with a nonzero baseline and wavelength of 24 (P values displayed on graphs), and as appropriate, a sine wave or horizontal line was plotted. **I** Mass cytometric analysis of short chain fatty acids in caecal samples across time. Values are normalised to set the metabolite median value to one, $n = 5$/time /condition. See also Supplementary Fig. 5 and Supplementary Table 1.

paradigms, sometimes termed "ultradian feeding" (where ultradian refers to a recurring rhythm with a period shorter than 24 h) or "spread-out feeding", have been used previously to abolish rhythmic food intake. Collectively, these studies have demonstrated impact on: peripheral gene expression over 24 h[31–33]; the central clock[34]; rhythmic parasite behaviour[35]; and longevity driven by caloric restriction[36]. The interval feeding paradigm utilised here effectively partitioned food consumption into regular, equally sized meals, and rhythms in food intake were effectively uncoupled from behavioural rhythms. However, as a caveat, we note that overall daily food intake was somewhat reduced for interval fed mice, and these animals did not gain weight during the experimental period, whilst ad libitum fed mice did.

IECs are highly rhythmic, with 36% of the transcriptome exhibiting 24 h oscillations under ad libitum fed conditions. Through the use of interval feeding, we demonstrated that diurnal rhythmicity in feeding behaviour is not required in order for the IEC clock to oscillate. This aligns with work demonstrating persistence of the hepatic molecular clock under a similar interval feeding regimen[31]. The IEC clock remained robustly rhythmic; both the positive and negative arms of the clockwork machinery exhibited phase advances (with no change in amplitude). It remains to be seen how clocks within additional cell types within the gut respond to interval feeding. Intriguingly, recent work has demonstrated both cell-type differences and regional differences in entrainment properties of clocks within intestinal cells[13]. Several rhythmic feeding-derived signals have demonstrated modulatory impact on the core clock. Amongst them are hormones such as insulin and insulin-like growth factor 1 (IGF-1)[28]; tryptophan metabolites[29]; and microbial metabolites such as SCFAs[30,41]. Thus, whilst diurnal rhythms in feeding are not required to maintain IEC clocks, our data implicates the importance of rhythmic feeding-derived cues for phase-setting and likely synchronisation of intrinsic clocks across multiple tissues. Although beyond the scope of this current study, a greater understanding of interactions between feeding-derived rhythmic signals and the core clock machinery across peripheral tissues is warranted.

Because the IEC intrinsic clock persisted under interval feeding, we were able to interrogate the importance of autonomous clocks on the IEC transcriptome independent of the acute effects of feeding. Approximately a quarter of all cycling transcripts under ad libitum conditions lost rhythmicity in IECs in response to interval feeding. This suggests significant dependence on signals derived from rhythmic food intake. Thus, the IEC clock has limited input to local transcriptional rhythmicity, and behavioural rhythms in feeding, driven by the central clock, provide a significant contribution. It remains to be seen whether this dominant influence of feeding behaviour persists in other peripheral tissues beyond the gut and liver. Our analysis highlighted lipids (sterols and cholesterol) and fatty acids (palmitic acid and palmitoleic acid) as upstream regulators of this subset of transcripts. Palmitate (an ester of palmitic acid) alters the circadian transcriptome via histone modification of enhancers[31] and thus presents as a viable feeding-derived signal important for driving rhythmicity in IECs independent of the clockwork machinery. Additionally, SREBF1/2 emerged as upstream transcriptional regulators of genes that lost rhythmicity. Expression and activity of these transcription factors exhibit robust 24 h oscillations in the liver, driven largely by sterol availability[37,39], but also via the core clock component REV-ERBα[42–45]. Thus, rhythms in sterol availability provide a further feeding-derived mechanism that could drive rhythmic transcription in the IEC independent of the core clockwork.

In the absence of diurnal feeding behaviour, we observed loss of rhythmicity within the microbiota. Prior work assessing the importance of feeding behaviour on the rhythmic microbiome has often relied on time-restricted feeding paradigms[20] or starvation[40]. Both approaches demonstrate significant impact; the former is associated with inversion of the molecular clock within peripheral tissues[46] (making it impossible to pick apart the relative contribution of feeding alone) and the latter is associated with metabolic stress. By uncoupling feeding behaviour and IEC clock activity, we reveal that feeding patterns have a profound effect on the rhythmicity of the gut bacteria, with interval feeding rendering 75% of the normally rhythmic OTUs arrhythmic.

The host immune system employs multiple mechanisms to orchestrate rhythms in the gut microbiota. This includes input from the IECs[40], intestinal IgA$^+$ plasma cells[22], and innate lymphoid cells (ILCs)[47]. Given that interval feeding was not associated with disruption to the molecular clock in the IEC or liver, we speculate that intrinsic clocks within ILCs and plasma cells are similarly unaffected. We propose that interval feeding disrupts microbial oscillations via perturbation of rhythms in the availability of nutrients, which influence IgA secretory activity of plasma cells. Our prior work has shown that feeding behaviour imprints rhythmicity onto the microbiome via rhythmic secretion of IgA by intestinal plasma cells, which is entrained by the timing of feeding and the resulting daily oscillations in nutrient availability[22]. One potential mechanism that warrants further exploration is the availability of dietary cholesterol. Oxysterols, such as 25-hydrocycholesterol (25HC), regulate plasma cell IgA production. Availability of 25HC to plasma cells is controlled by IEC expression of cholesterol 25-hydroxylase (CH25H), which facilitates the generation of oxysterols from cholesterol[48,49]. Interestingly, we previously demonstrated cholesterol biosynthesis pathways to be highly rhythmic in intestinal IgA+ plasma cells, while IgA secretion was determined by the time of feeding[22]. Thus, the striking loss of IgA rhythmicity observed under interval feeding could be driven by altered rhythmicity in cholesterol availability or altered cholesterol handling in IECs. This remains to be directly tested, and it is important that future work considers the small intestine, given that this region is the major site of nutrient absorption and IgA production, and takes into consideration the differences in microbial communities along the length of the GI tract.

In line with the loss of 24 h rhythmicity in IgA, 24 h oscillations were lost in key commensals. This included the Firmicutes, *Oscillobacter* and *Lactobacillus gasseri*. *Oscillobacter* rhythms were damped, with reduced relative abundance during the late night (ZT20-ZT0) in interval-fed mice. *Oscillobacter* metabolise cholesterol, and in humans, a high abundance of this microbe is associated with lower cholesterol levels[50], suggesting that the observed damped rhythms might result in altered rhythms in cholesterol metabolism. The observed loss of rhythmicity in microbial populations in the absence of diurnal feeding-fasting behaviour has important implications for metabolic health. In mice, rhythmic microbial function modulates time-of-day differences in metabolite availability and uptake by the host, and is important for driving rhythmic blood glucose levels[22]. Further, in humans, an arrhythmic microbiome is associated with increased risk of type 2 diabetes[21]. Microbiome rhythmicity also has important implications for

the maintenance of immunity. For example, a rhythmic microbiome is required for immune homoeostasis in the gut[6]. Furthermore, rhythmic microbial metabolites imprint rhythmicity onto inflammatory disease[23].

This study set out to establish a foundational understanding of how loss of rhythmic feeding behaviour impacts 24 h rhythms within the gastrointestinal tract. We acknowledge that the interval feeding regimen utilised to address this goal does come with some limitations. Unfortunately, because mice were co-housed, we were unable to record food intake for each individual mouse at each meal. Whilst food intake assessed by cage suggests limited impact on total calorie consumption, we cannot completely rule out the notion that some individual mice may have experienced a degree of caloric restriction, with potential impact on stress, clock mechanisms, microbiota rhythmicity and metabolic state, which could confound interpretation of these data. Furthermore, although beyond the scope of this study, it would be of interest to explore how this interval feeding influences daily rhythms in metabolism. Assessing impact on gut-derived hormones (including glucagon-like peptide-1 and ghrelin), glucose and insulin will inform on the relative importance of food timing and clock status on these rhythmic parameters.

In summary, this study highlights the importance of food timing for the maintenance of 24 h rhythms in gut homoeostasis. Feeding-derived signals are important for the maintenance of daily rhythms within the IEC transcriptome, independent of the function of the IEC intrinsic clock. Interval feeding resulted in loss of 24 h rhythmicity in IgA secretion, which was associated with loss of rhythmicity in a number of commensal bacteria and their metabolic outputs. Such loss of rhythmicity in the microbiome has been associated with aberrant metabolic and immune health. Together, these data highlight the importance of considering both "what we eat" and "when we eat" for maintenance of gut immune and metabolic health. Lifestyle factors including: chronotype (an individual's natural preference to sleep and wake at certain times of the day); shift-work; and intermittent fasting all influence feeding behaviour, and the impact of this should be considered. Shift work is associated with both metabolic disease and chronic inflammatory disease[51–55]. This is often linked to disrupted sleep timing and quality; our study provides support for the contribution of disrupted feeding behaviour to ill health associated with shift work[56]. Modification of meal timing presents an attractive, cost-effective and accessible behavioural intervention that may have benefits on health. Such interventions could have potential application in the management of adverse health consequences associated with shift-work or age-related changes in circadian function.

Methods

Animals

All experimental procedures were performed in accordance with the UK Animals (Scientific Procedures) Act 1986, subject to local ethical review and approval from the University of Manchester Animals Welfare and Ethical Review Body (AWERB). Mice were housed in the Biological Services Facility (BSF) at the University of Manchester with regulated temperature (19–23 °C) and humidity (45–65%). Mice were housed under a 12:12 light:dark cycle in light-controllable cabinets, whereby zeitgeber time 0 (ZT0) refers to lights on, and ZT12 refers to lights off. 8–12-week-old male C57BL/6J mice (Charles River Laboratories) were used and were co-housed. Mice were provided with ad libitum access to water. Mice were randomly assigned to a feeding regimen, either standard chow was provided ad libitum or via the interval feeding paradigm described below. Animals were provided with Sizzle-Nest and environmental enrichment in the form of shelters, gnawing sticks and cardboard tubes. At the end of the feeding regimen, animals were sacrificed using a Schedule 1 method (cervical dislocation in the absence of anaesthesia). Terminal blood and samples of colon, liver, faeces and caecum were collected and processed as described below. Sample analysis via flow cytometry, QPCR, ELISA and mass spectrometry was performed with the operator blinded to the origin of the sample.

Interval feeding

Food availability was restricted to a short feeding window every 3 h. Upon initiating the interval feeding regimen, during the 4 meals in the light phase (ZT2, ZT5, ZT8 and ZT11) food hoppers were made available for a 30 min window. For the 4 meals during the dark phase (ZT14, ZT17, ZT20 and ZT23), food hoppers were made available for a 10 min window. On the fifth day onwards (in response to observations that mice were consuming more food during the mealtime immediately after lights on, compared to later mealtimes during the light phase), the ZT2 meal was reduced to 20 min, and the dark phase meals were increased to 12.5 min to maintain equal light and dark food intake. Food was weighed after each feeding window, providing a total per cage, and this was divided by the number of mice in the cage ($n = 5$) to provide daily food intake/mouse. Animal body weight was tracked daily. Food was delivered manually or using a programmable automated system (TSE systems). Large intact food pellets were provided during meals to avoid smaller fragments falling onto the cage floor, and cages were regularly checked to ensure there was no residual food on the floor.

Analysis of metabolic parameters

Following a 2-week period of interval feeding (or for controls, ad libitum feeding) in standard individual ventilated cages, mice were transferred to the PhenoMaster (TSE systems) for analysis of metabolic and behavioural parameters. Here, mice were singly housed within a light-tight cabinet. All mice were provided with Sizzle-Nest and a shelter and had free access to drinking water. For interval fed animals ($n = 6$), the food hopper was filled for the duration of the mealtimes and then emptied (ensuring no food had escaped onto the cage floor). Control mice had ad libitum access to food ($n = 5$), but hoppers were agitated during the interval fed animals' mealtimes to ensure consistency. The PhenoMaster captured data every 2 min including water consumption, activity (infra-red activity frame), oxygen consumption and carbon dioxide production. Animals were allowed to acclimatise for 15 h before data were collected for analysis.

Colonic IEC isolation

Colonic IECs were extracted using established methods[6]. In brief, dissected colons were opened out longitudinally and sectioned into four pieces, washed in ice-cold PBS and incubated in PBS containing 2% FBS on ice. After 20 min, the tissue was transferred to HBSS containing 2 mM EDTA and 1 mM dithiothreitol and placed in a shaking incubator (180 rpm, 37 °C, 15 min). Subsequently, samples were vigorously agitated for 30 s to dissociate the epithelium from the basement membrane before being passed through a 70 µm filter. The effluent was centrifuged (432×*g*, 4 °C, 5 min) and the pellet, containing IECs, resuspended in 350 µL RLT plus buffer (Qiagen) and stored at −20 °C. RNA was extracted using the RNeasy Plus Mini Kit (Qiagen) according to the manufacturer's instructions. For purity checks, isolated colonic cells were stained with PE-labelled EpCAM (G8.8, eBioscience) and BV510-labelled CD45 (30-F11, Biolegend) 1:200 following a 20 min Fc block (anti-mouse CD16/CD32 eBioscience, 1:100). Cells were washed with and then resuspended in FACS buffer (PBS + 5% FBS) before analysis on a BD LSR II.

Liver RNA extraction

Liver tissue was homogenised in Trizol using Lysing Matrix D tubes and a BeadMill homogeniser (Fisher Scientific). RNA was extracted using chloroform, then precipitated using isopropanol. After washing in 70% ethanol, the RNA pellet was resuspended in RNase-free water.

QPCR

RNA was quantified (NanoDrop, Thermo Fisher Scientific) and converted to cDNA using High-Capacity RNA to cDNA kits (ThermoFisher). Taqman primers and probes (see Supplementary Table 2) were utilised, and plates were run on a QuantStudio 1 machine (Applied Biosystems) using Takyon ROX probe 2X qPCR MasterMix dTTP blue (Eurogentec Ltd). β-actin was utilised as a housekeeping gene.

RNA sequencing

RNA was extracted from IECs, and quality was determined using a 2200 TapeStation (Agilent Technologies). Library preparation and sequencing were performed by the University of Manchester Genomic Technologies Core Facility. Libraries were generated using the TruSeq Stranded mRNA assay (Illumina) according to the manufacturer's protocol. Multiplexed libraries were analysed by paired-end sequencing on a HiSeq 4000 instrument (76 + 76 cycles, plus indices), then de-multiplexed and converted using bcl2fastq software (v2.17.1.14, Illumina). Adaptors were removed and ends were trimmed using Trimmomatic (v0.36). Reads were mapped against the mouse genome (mm10/GRCm38) using STAR (v2.5.3). Reads were then counted, normalised and annotated in R using the Rsubread (v1.28.1), edgeR (v3.30.3) and biomaRt (v2.44.0) packages. One sample was excluded from further analysis from the ad libitum fed ZT20 group as it did not meet our quality control standards (leaving $n = 4$ in this group). Differential expression analysis was run in RStudio using edgeR (v3.28.1). Genes were differentially expressed (DE) if the false discovery rate (FDR) was <0.05 and log2-fold change of <−2 or >2. Rhythmicity analysis was performed in RStudio using the CompareRhythms package[57]. CompareRhythms uses a model selection approach and compares how well models with different patterns of rhythmicity fit the data from the two treatment groups, to classify genes either as "arrhythmic" or "rhythmic" in at least one condition with a "gain", "loss", "change" or the "same" rhythmicity between conditions (reporting phase and amplitude where appropriate). Where the rhythmicity in transcript expression is determined to be the "same" between the treatment groups, this generates a single fit across both datasets and therefore shared amplitude and phase. Pathway analysis of sets of genes was performed using Enrichr and the mouse KEGG 2019 database. Expression of individual genes contributing to specific pathways (irrespective of their rhythmicity status) graphed as spline plots are available in Supplementary Data 2.

16 s rRNAseq

Faecal pellets were collected from the terminal end of the colon (1–2 pellets/mouse), snap-frozen in liquid nitrogen and stored at −80 °C. Bacterial DNA was extracted from a 250 mg sample using the Powersoil kit (Qiagen, Germany) according to the manufacturer's instructions. DNA was eluted in the final step using a 50 µl volume. DNA was quantified using a Nanodrop 2000 (Thermo Fisher Scientific) using a 260/280 purity threshold > 1.8. and normalised across all samples. 20 µL of DNA (1 ng/µl) was sequenced using primers spanning the variable region 2 (V4) of the 16s rRNA gene[8] by the University of Liverpool Centre for Genomic Research using the Illumina MiSeq v2 platform (Illumina) to generate 250 bp paired end reads. Raw FastQ files were trimmed and reads <15 bp were discarded. The trimmed FastQ files were then processed using the 16S Amplicon Analysis pipeline in Centaurus Galaxy Server (University of Manchester Bioinformatics Core Facility), generating OTU tables. Briefly, reads were paired, OTUs were clustered using VSEARCH, and chimeric sequences were removed. The resulting OTU data were mapped onto taxonomies using the Silva reference database (v138) with a sequence homology threshold of >97%. The generated OTU biom table was subsequently analysed in R Studio using the Phyloseq package (V1.38.0)[58], which enabled the extraction of information on total and relative taxonomic abundances, as well as the assessment of alpha diversity, using the Shannon Index. Rhythmicity analysis of OTUs and taxonomies was performed using JTK_cycle[59] of MetaCycle (v1.2.0), with period length fixed to 24 h. OTUs were determined to be significantly rhythmic if the Adj.$P < 0.05$.

Corticosterone ELISA

Terminal blood was collected in MiniCollect K3EDTA tubes (Greiner Bio-One) and stored on ice prior to centrifugation (3000×*g*, 4 °C, 10 min). Plasma was transferred to cryovials and flash frozen in liquid nitrogen. Plasma corticosterone levels were determined by ELISA (Enzo Life Sciences, Inc.) following the manufacturer's instructions. Absorbance values were determined using the Promega GloMax plate reader at 405 nm.

IgA ELISA

For assessment of IgA, faecal pellets were collected from the terminal end of the colon (1–2 pellets/mouse), snap-frozen in liquid nitrogen and stored at −80 °C. Samples were prepared for analysis by homogenisation in PBS. Pellets were transferred to lysing matrix tubes (MP Biomedicals), resuspended in PBS (100 mg/ml) and homogenised using a Bead Mill 24 Homogeniser (Fisher Scientific). Samples were centrifuged (200×*g*, 1 min) and the supernatant diluted (1 mg/ml) before further centrifugation 3 times for 5 min at 200×*g*, 8000×*g* and 10,000×*g*, removing the pellet each time. The final supernatant was further diluted 1:4 in preparation for analysis. Faecal IgA concentration was determined by an ELISA (Bethyl Laboratories) following the manufacturer's instructions.

SCFA analysis

Caecal contents were snap frozen and stored at −80 °C prior to analysis. Samples were resuspended 1:10 (based on weight of sample) in nuclease-free water and transferred to lysing matrix D tubes (MP Biomedicals) for homogenisation using a BeadMill homogeniser. Homogenised samples were centrifuged (18,800×*g*, 5 min, 4 °C) and supernatant stored at −80 °C. To quantify levels of SCFAs, targeted metabolomics was performed using liquid chromatography–mass spectrometry (LC–MS; Mass Spectrometry Core Research Facility at the University of Manchester). LC–MS analysis was performed using a SCIEX Exion LC system consisting of two AD high-pressure gradient pumps, vacuum degasser, solvent valve, AC column oven and AC autosampler, coupled to a SCIEX 7600 ZenoTOF Q-TOF mass spectrometer with TurboV optiflow ion source running a 50 µm ESI probe. The system was controlled by SCIEX OS v3.0. For each sample, an area ratio was calculated using the peak area of an internal standard (in order to correct for any batch effects) and this was normalised to the median value of all samples.

Statistical analysis

Each individual animal was considered an experimental unit. Feeding experiments (in the absence of the Phenomaster system) were powered to allow $n = 5$ mice per time point ($n = 30$/feeding regimen). Where sample collection failed (e.g. terminal blood collection for corticosterone ELISA) or sample processing failed (e.g. protein extraction from faecal pellets and purification of colonic IECs) the modified n numbers are presented in the figure legends. Statistical tests were conducted in GraphPad Prism and are specified in the figure legends where appropriate. Throughout * denotes $p < 0.05$; ** $p < 0.01$ and ***$p < 0.005$.

Data availability

The IEC RNAseq dataset generated during the current study is available at ArrayExpress (accession code E-MTAB-14883) as of the date of publication. 16s rRNA seq data generated during the current study are not publicly available but are available from the corresponding author on reasonable request. Requests for further information and resources should be directed to and will be fulfilled by the lead contact, Julie Gibbs (Julie.gibbs@manchester.ac.uk). This study did not generate new, unique reagents.

Received: 4 September 2025; Accepted: 4 June 2026;
Published online: 22 June 2026

References

1. Ashton, A., Foster, R. G. & Jagannath, A. Photic entrainment of the circadian system. *Int. J. Mol. Sci.* **23**, 729 (2022).
2. Schibler, U. et al. Clock-talk: interactions between central and peripheral circadian oscillators in mammals. *Cold Spring Harb. Symp. Quant. Biol.* **80**, 223–232 (2015).
3. Cox, K. H. & Takahashi, J. S. Circadian clock genes and the transcriptional architecture of the clock mechanism. *J. Mol. Endocrinol.* **63**, R93–R102 (2019).

4. Patton, A. P. & Hastings, M. H. The mammalian circadian time-keeping system. *J. Huntingt. Dis.* **12**, 91–104 (2023).
5. Hibberd, T. J. et al. Circadian rhythms in colonic function. *Front. Physiol.* **14**, 1239278 (2023).
6. Tuganbaev, T. et al. Diet diurnally regulates small intestinal microbiome–epithelial–immune homeostasis and enteritis. *Cell* **182**, 1441–1459 e1421 (2020).
7. Brooks, J. F. et al. The microbiota coordinates diurnal rhythms in innate immunity with the circadian clock. *Cell* **184**, 4154–4167 e4112 (2021).
8. Simpkins, D. A. et al. Consequences of collagen induced inflammatory arthritis on circadian regulation of the gut microbiome. *FASEB J.* **37**, e22704 (2023).
9. Thaiss, C. A. et al. Microbiota diurnal rhythmicity programs host transcriptome oscillations. *Cell* **167**, 1495–1510 e1412 (2016).
10. Tognini, P. et al. Distinct circadian signatures in liver and gut clocks revealed by ketogenic diet. *Cell Metab.* **26**, 523–538 e525 (2017).
11. Weger, B. D. et al. The mouse microbiome is required for sex-specific diurnal rhythms of gene expression and metabolism. *Cell Metab.* **29**, 362–382 e368 (2019).
12. Dantas Machado, A. C. et al. Diet and feeding pattern modulate diurnal dynamics of the ileal microbiome and transcriptome. *Cell Rep.* **40**, 111008 (2022).
13. Magana, I. et al. Not all gut cellular circadian oscillators are food entrainable. *Proc. Natl. Acad. Sci. USA*. **123**, e2601012123 (2026).
14. Niu, Y. et al. Targeting the intestinal circadian clock by meal timing ameliorates gastrointestinal inflammation. *Cell. Mol. Immunol.* **21**, 842–855 (2024).
15. Okumura, R. & Takeda, K. Roles of intestinal epithelial cells in the maintenance of gut homeostasis. *Exp. Mol. Med.* **49**, e338 (2017).
16. Butler, T. D. & Gibbs, J. E. Circadian host–microbiome interactions in immunity. *Front. Immunol.* **11**, 1783 (2020).
17. Zarrinpar, A., Chaix, A., Yooseph, S. & Panda, S. Diet and feeding pattern affect the diurnal dynamics of the gut microbiome. *Cell Metab.* **20**, 1006–1017 (2014).
18. Liang, X., Bushman, F. D. & FitzGerald, G. A. Rhythmicity of the intestinal microbiota is regulated by gender and the host circadian clock. *Proc. Natl. Acad. Sci. USA*. **112**, 10479–10484 (2015).
19. Leone, V. et al. Effects of diurnal variation of gut microbes and high-fat feeding on host circadian clock function and metabolism. *Cell Host Microbe* **17**, 681–689 (2015).
20. Thaiss, C. A. et al. Transkingdom control of microbiota diurnal oscillations promotes metabolic homeostasis. *Cell* **159**, 514–529 (2014).
21. Reitmeier, S. et al. Arrhythmic gut microbiome signatures predict risk of type 2 diabetes. *Cell Host Microbe*. **28**, 258–272 e256 (2020).
22. Penny, H. A. et al. Rhythmicity of intestinal IgA responses confers oscillatory commensal microbiota mutualism. *Sci. Immunol.* **7**, eabk2541 (2022).
23. Ma, F. et al. Dietary-timing-induced gut microbiota diurnal oscillations modulate inflammatory rhythms in rheumatoid arthritis. *Cell Metab.* **37**, 1454 (2025).
24. Gagliano, O. et al. Synchronization between peripheral circadian clock and feeding-fasting cycles in microfluidic device sustains oscillatory pattern of transcriptome. *Nat. Commun.* **12**, 6185 (2021).
25. Damiola, F. et al. Restricted feeding uncouples circadian oscillators in peripheral tissues from the central pacemaker in the suprachiasmatic nucleus. *Genes Dev.* **14**, 2950–2961 (2000).
26. Stokkan, K. A., Yamazaki, S., Tei, H., Sakaki, Y. & Menaker, M. Entrainment of the circadian clock in the liver by feeding. *Science* **291**, 490–493 (2001).
27. Vollmers, C. et al. Time of feeding and the intrinsic circadian clock drive rhythms in hepatic gene expression. *Proc. Natl. Acad. Sci. USA*. **106**, 21453–21458 (2009).
28. Crosby, P. et al. Insulin/IGF-1 drives PERIOD synthesis to entrain circadian rhythms with feeding time. *Cell* **177**, 896–909 e820 (2019).
29. Petrus, P. et al. Tryptophan metabolism is a physiological integrator regulating circadian rhythms. *Mol. Metab.* **64**, 101556 (2022).
30. Tahara, Y. et al. Gut microbiota-derived short chain fatty acids induce circadian clock entrainment in mouse peripheral tissue. *Sci. Rep.* **8**, 1395 (2018).
31. Greenwell, B. J. et al. Rhythmic food intake drives rhythmic gene expression more potently than the hepatic circadian clock in mice. *Cell Rep.* **27**, 649–657 e645 (2019).
32. van der Veen, D. R. et al. Impact of behavior on central and peripheral circadian clocks in the common vole Microtus arvalis, a mammal with ultradian rhythms. *Proc. Natl. Acad. Sci. USA*. **103**, 3393–3398 (2006).
33. Mange, F. et al. Diurnal regulation of RNA polymerase III transcription is under the control of both the feeding-fasting response and the circadian clock. *Genome Res.* **27**, 973–984 (2017).
34. Sen, S. et al. Ultradian feeding in mice not only affects the peripheral clock in the liver, but also the master clock in the brain. *Chronobiol. Int.* **34**, 17–36 (2017).
35. Rijo-Ferreira, F. et al. The malaria parasite has an intrinsic clock. *Science* **368**, 746–753 (2020).
36. Acosta-Rodriguez, V. et al. Circadian alignment of early onset caloric restriction promotes longevity in male C57BL/6J mice. *Science* **376**, 1192–1202 (2022).
37. Matsumoto, E. et al. Time of day and nutrients in feeding govern daily expression rhythms of the gene for sterol regulatory element-binding protein (SREBP)-1 in the mouse liver. *J. Biol. Chem.* **285**, 33028–33036 (2010).
38. Brewer, M., Lange, D., Baler, R. & Anzulovich, A. SREBP-1 as a transcriptional integrator of circadian and nutritional cues in the liver. *J. Biol. Rhythms* **20**, 195–205 (2005).
39. Gilardi, F. et al. Genome-wide analysis of SREBP1 activity around the clock reveals its combined dependency on nutrient and circadian signals. *PLoS Genet.* **10**, e1004155 (2014).
40. Heddes, M. et al. The intestinal clock drives the microbiome to maintain gastrointestinal homeostasis. *Nat. Commun.* **13**, 6068 (2022).
41. Fawad, J. A. et al. Histone deacetylase inhibition by gut microbe-generated short-chain fatty acids entrains intestinal epithelial circadian rhythms. *Gastroenterology* **163**, 1377–1390 e1311 (2022).
42. Le Martelot, G. et al. REV-ERBalpha participates in circadian SREBP signaling and bile acid homeostasis. *PLoS Biol.* **7**, e1000181 (2009).
43. Wang, X., Sato, R., Brown, M. S., Hua, X. & Goldstein, J. L. SREBP-1, a membrane-bound transcription factor released by sterol-regulated proteolysis. *Cell* **77**, 53–62 (1994).
44. Shimomura, I. et al. Cholesterol feeding reduces nuclear forms of sterol regulatory element binding proteins in hamster liver. *Proc. Natl. Acad. Sci. USA*. **94**, 12354–12359 (1997).
45. Cyster, J. G., Dang, E. V., Reboldi, A. & Yi, T. 25-Hydroxycholesterols in innate and adaptive immunity. *Nat. Rev. Immunol.* **14**, 731–743 (2014).
46. Sladek, M. et al. Insight into the circadian clock within rat colonic epithelial cells. *Gastroenterology* **133**, 1240–1249 (2007).
47. Godinho-Silva, C. et al. Light-entrained and brain-tuned circadian circuits regulate ILC3s and gut homeostasis. *Nature* **574**, 254–258 (2019).
48. Trindade, B. C. et al. The cholesterol metabolite 25-hydroxycholesterol restrains the transcriptional regulator SREBP2 and limits intestinal IgA plasma cell differentiation. *Immunity* **54**, 2273–2287 e2276 (2021).
49. Ceglia, S. et al. An epithelial cell-derived metabolite tunes immunoglobulin A secretion by gut-resident plasma cells. *Nat. Immunol.* **24**, 531–544 (2023).

50. Li, C. et al. Gut microbiome and metabolome profiling in Framingham Heart Study reveals cholesterol-metabolizing bacteria. *Cell* **187**, 1834–1852 e1819 (2024).
51. Maidstone, R. J. et al. Night shift work is associated with an increased risk of asthma. *Thorax* **76**, 53–60 (2021).
52. Faraut, B. et al. Immune disruptions and night shift work in hospital healthcare professionals: the intricate effects of social jet-lag and sleep debt. *Front. Immunol.* **13**, 939829 (2022).
53. Loef, B. et al. Immunological effects of shift work in healthcare workers. *Sci. Rep.* **9**, 18220 (2019).
54. Bayon, V. et al. Impact of night and shift work on metabolic syndrome and its components: a cross-sectional study in an active middle-to-older-aged population-based sample. *BMJ Open* **12**, e053591 (2022).
55. Soltanzadeh, A. et al. Investigating the relationship between shift work schedule and blood and metabolic parameters: a 10-years retrospective cohort study. *Sci. Rep.* **14**, 17297 (2024).
56. Erickson, M. L. et al. Nightshift imposes irregular lifestyle behaviors in police academy trainees. *Sleep Adv.* **4**, zpad038 (2023).
57. Pelikan, A., Herzel, H., Kramer, A. & Ananthasubramaniam, B. Venn diagram analysis overestimates the extent of circadian rhythm reprogramming. *FEBS J.* **289**, 6605–6621 (2022).
58. McMurdie, P. J. & Holmes, S. phyloseq: an R package for reproducible interactive analysis and graphics of microbiome census data. *PLoS ONE* **8**, e61217 (2013).
59. Hughes, M. E., Hogenesch, J. B. & Kornacker, K. JTK_CYCLE: an efficient nonparametric algorithm for detecting rhythmic components in genome-scale data sets. *J. Biol. Rhythms* **25**, 372–380 (2010).

Acknowledgements

We would like to thank Andy Hayes and the University of Manchester Genomics Core Technology Facility and Leo Zeef and the University of Manchester Bioinformatics Core Facility. We are grateful for the help received from Dr. George Taylor and the University of Manchester Biological Mass Spectrometry Core Facility. 16s rRNA sequencing was performed by the University of Liverpool Centre for Genomics Research. We would like to thank David Bechtold for his expert advice on indirect calorimetry and for providing insightful feedback on drafts of the manuscript. We thank the University of Manchester Biological Sciences Facility staff for support with animal husbandry and maintenance, and the University of Manchester Flow Facility. F.K.H was funded by an MRC doctoral training programme award. J.E.G. is a Versus Arthritis Senior Fellow (22625). M.R.H. is supported by a Wellcome Trust Sir Henry Dale Fellowship (105644/Z/14/Z).

Author contributions

Conceptualisation: J.E.G., M.R.H. and K.J.E.; Methodology: F.K.H. and J.E.G.; Investigation: F.K.H., P.D., A.L.M., S.D., J.C. and J.E.G.; Resources: J.E.G.; Writing—original draft: F.K.H. and J.E.G.; Writing— review and editing: F.K.H., K.J.E., M.R.H., P.D. and J.E.G.; Visualisation: F.K.H., P.D. and J.E.G.; Supervision: K.J.E., M.R.H. and J.E.G.; Project administration: F.K.H. and J.E.G.; Funding acquisition: F.K.H., K.J.E., M.R.H. and J.E.G. All authors read and approved the final manuscript.

Competing interests

The authors declare no competing interests.

Additional information

Supplementary information The online version contains supplementary material available at https://doi.org/10.1038/s44323-026-00089-x.

Correspondence and requests for materials should be addressed to Julie E. Gibbs.